3

4

5   **Metabolomic Study of Stress Responses Leading to Plant Resistance**

6   **in Mandarin Fruit Mediated by Preventive Applications of *Bacillus***

7   ***subtilis* Cyclic Lipopeptides**

8

9

10   Paiboon Tunsagool[a,*], Xiaohang Wang[b,*], Wichitra Leelasuphakul[a], Warangkana

11   Jutidamrongphan[c,**], Narumon Phaonakrop[d], Janthima Jaresitthikunchai[d], Sittiruk Roytrakul[d],

12   Guanqun Chen[e], and Liang Li[b,**]

13

14   [a]Department of Biochemistry, [c]Faculty of Environmental Management, Prince of Songkla

15   University, Songkhla 90112, Thailand.

16   [b]Department of Chemistry, University of Alberta, Edmonton, Alberta T6G 2G2, Canada.

17   [d]Proteomics Research Laboratory, National Center for Genetic Engineering and

18   Biotechnology, National Science and Technology Development Agency, Thailand Science

19   Park (TSP), Pathum Thani 12120, Thailand.

20   [e]Department of Agricultural, Food and Nutritional Science, University of Alberta, Edmonton,

21   Alberta T6G 2P5, Canada.

22   [*]Co-first author

23   [**]To whom correspondence should be addressed. Warangkana Jutidamrongphan: E-mail

24   address: warangkana.j@psu.ac.th; Tel: +66 74 386844; Fax +66 74 429758; Liang Li: E-mail

25   address: liang.li@ualberta.ca; Tel: +1 780 4923250; Fax +1 780 4928231

26 **ABSTRACT**

27   Although green mold rot caused by *Penicillium digitatum* is a major postharvest disease in

28 mandarin fruit, the fruit's defense mechanism at the metabolomic level is largely unknown.

29 Here, the expressed metabolome network leading to plant resistance to stresses induced by

30 exposing of different agents was analyzed. Inoculation of mandarin fruits with eight

31 individual agents, including four *Bacillus* cyclic lipopeptides (CLPs) produced by *B. subtilis*

32 ABS-S14, three phytohormones and *P. digitatum,* resulted in different wound appearance on

33 flavedo (mandarin peel) tissues. Subsequent metabolomic analysis with dansylation isotope

34 labeling LC-MS method detected and quantified 4,717 metabolites, including 77 metabolites

35 positively identified belonging to 39 metabolic pathways. The preventive applications of

36 CLPs showed the greatest effect with many up-regulated metabolite changes in fruit tissues,

37 including two important secondary metabolites, serotonin and tyramine, which were reported

38 to stimulate plant defensive system during stress. Further analysis indicated that CLPs

39 triggered the metabolism of glycine, serine and threonine, a major pathway to induce

40 serotonin production, and activated tyrosine metabolism resulting in an increase of tyramine

41 production. These findings provide the new insights for fruit protection manipulation from

42 green mold pathogen invasion during postharvest storage.

43

46

1. Introduction

Green mold rot caused by *Penicillium digitatum* is a major factor in economic loss of citrus fruit (Eckert, 1978). The infection of *P. digitatum* generally occurs on the pores or wound sites on mandarin peel during postharvest period (Palou et al., 2008). Synthetic fungicides have been used in the prevention and treatment of *P. digitatum* infection, but consumers are more concerning about their negative effects on environment and human health (Talibi et al., 2014). Identification and use of safer biological control agents to reduce rot during the postharvest period therefore has the potential to be a feasible strategy to overcome the limitations inherent in the usage of synthetic fungicides (Palou et al., 2008; Talibi et al., 2014).

Microbial compounds such as cyclic lipopeptides (CLPs) isolated from *Bacillus* species have been exploited as biological control agents to restrict plant pathogen invasion (Ongena and Jacques, 2008; Rosier et al., 2018). *B. subtilis* can not only elicit plant defense responses, but also act as an alternative agent to replace pesticide usage for the control of green mold disease in citrus fruit (Leelasuphakul et al., 2008; Waewthongrak et al., 2015). For instance, an antagonistic strain *B. subtilis* ABS-S14 was recently reported to produce CLPs consisting of three main families (i.e., fengycins, iturins and surfactins), which manifested strong antifungal activities against *P. digitatum* and induced resistance in citrus fruit (Waewthongrak et al., 2014). Moreover, CLPs of *Bacillus subtilis* were shown to be involved in complex regulatory processes of host plant immunity such as induced systemic resistance system (Ongena and Jacques, 2008).

In addition to CLPs, plant phytohormones have also been studied for their potential as biological control agents to inhibit plant pathogen infection (Guo et al., 2014; Moscoso-Ramírez and Palou, 2013). Potent exogenous plant hormones such as salicylic acid (SA), methyl jasmonate (MeJA) and ethephon (Et) involve in SA, jasmonic acid and ethylene

72 signaling transduction pathways during plant defense responses, respectively (Guo et al.,

73 2014; John-Karuppiah and Burns, 2010; Moscoso-Ramírez and Palou, 2013; Vlot et al.,

74 2009; Zhou et al., 2018). Preventive applications of SA and MeJA could inhibit the green

75 mold disease in citrus fruit (Guo et al., 2014; Moscoso-Ramírez and Palou, 2013). Et could

76 induce the expression of *1-amino-cyclopropane-1-carboxylate synthase-1* and *1-amino-*

77 *cyclopropane-1-carboxylate oxidase* genes in the ethylene signaling pathway, which is

78 related to the induced systemic resistance system in sweet orange (John-Karuppiah and Burns,

79 2010).

80   As potential biological control agents, *Bacillus* CLPs and plant hormones offer different

81 extent of protection to the citrus fruits against green mold pathogen (Guo et al., 2014;

82 Moscoso-Ramírez and Palou, 2013; Waewthongrak et al., 2015). During postharvest period,

83 metabolic changes induced by *Bacillus* CLPs and phytohormones in mandarin fruit occurred

84 in response to stresses such as wound stress, which could induce plant immunity through the

85 induced systemic resistance system (Tunsagool et al., 2019). Since *P. digitatum* infects citrus

86 fruit from the wound sites (Eckert, 1978), this mold would also induce plant immunity in a

87 similar way (Ballester et al., 2013). If preventive application of CLPs or exogenous plant

88 hormones can effective stimulate wound recovery of citrus fruit's peel and plant immunity

89 against pathogen defense, this approach would effectively prevent green mold infection.

90 Therefore, in order to develop an effective method of using these biological control agents,

91 especially the bioactive *Bacillus* CLP compounds, to prevent green mold infection, it is

92 critical to investigate if these agents can stimulate wound healing of citrus fruit's peel and to

93 explore how these agents regulate metabolites against wound stress and related pathogen

94 defense responses in citrus fruit.

95   Metabolomics is a key technology to profile the metabolites in metabolic pathways (Guo

96 and Li, 2009; Huan et al., 2015; Shen et al., 2016). Metabolomics is also a powerful approach

97   to expand the knowledge of plant defense mechanism through signaling pathways by

98   determination of the metabolites which occurred in specific metabolic networks and stress

99   responses of plant (Hall et al., 2002). Metabolomics has been used to investigate primary and

100   secondary metabolites to monitor and assess gene function (Asai et al., 2017; Hall et al.,

101   2002; Sampaio et al., 2016). It has also been used to characterize post-genomic processes

102   from a broad perspective (Tugizimana et al., 2013), and to find biomarker candidates during

103   defense responses in citrus leaves (Asai et al., 2017). Based on gas chromatography mass

104   spectrometry (GC-MS) and statistical analysis, Asai et al. (2017) reported the involvement of

105   tryptophan and serine regulation in stress responses in citrus leaves when being wounded and

106   exposed to MeJA and SA. With the recent development of high-performance chemical

107   isotope labeling (CIL) liquid chromatography mass spectrometry (LC-MS), it is now possible

108   to quantify the metabolomic changes of biological systems with high metabolic coverage and

109   high quantification accuracy, thereby allowing the possibility of revealing up- and down-

110   regulated metabolites in many metabolic pathways.

111   In this study, we examined the wound recovery outcome of mandarin fruit responding to

112   various agents applied on the wound surface of flavedo, including *B. subtilis* CLPs and

113   exogenous phytohormones, and compared with green mold pathogen infection. In order to

114   better understand the CLPs' action on induction of host plant resistance, the metabolic

115   changes induced by different agents applied to citrus fruit were analyzed using metabolomics.

116   Dansylation LC-MS was applied to profile the metabolomic differences of the wound tissues

117   to examine metabolic responses, in particular, the defense response pathways.

118   **2. Materials and methods**

119   *2.1. Chemicals and reagents*

120   SA, MeJA and Et used as exogenous plant hormones were purchased from Sigma-Aldrich

121   and solutions were prepared in 80% ethanol. For dansylation labeling, ^{12}C-dansyl chloride

122   was purchased from Sigma-Aldrich and ^{13}C-dansyl chloride was synthesized according to a

123   previous study (Guo and Li, 2009). LC-MS grade water, methanol and acetonitrile were

124   purchased from Thermo Fisher Scientific (Alberta, Canada). All other chemicals and reagents

125   were purchased from Sigma-Aldrich Canada (Ontario, Canada).

126   *2.2. Plant materials*

127   Mandarin fruit (*Citrus reticulata* Blanco cv. Shogun) of uniform size and color without

128   physical injuries or infections were selected from the commercial orchards located in Loei

129   province of northeastern Thailand. The citrus plants were grown under organic control with

130   non-postharvest treatment applied. The fruit were surface-sterilized with 1% sodium

131   hypochlorite solution for 5 min and then allowed to air dry at 25°C (Waewthongrak et al.,

132   2015).

133   *2.3. Microorganisms*

134   *P. digitatum* was isolated from decayed mandarin fruit (Leelasuphakul et al., 2008). It was

135   identified microbiologically and collected in the Fungal Biodiversity Laboratory, National

136   Center for Genetic Engineering and Biotechnology, National Science and Technology

137   Development Agency, Thailand. A pure culture was placed on a potato dextrose agar (PDA)

138   plate and incubated at 24°C for 7 days. To maintain their pathogenicity, the fungal spores

139   were routinely inoculated back into mandarin fruit. The *P. digitatum* spore suspension was

140   prepared from a 7-day-old culture and a haemacytometer was used to adjust it to 10^7 spores

141   L^{-1} (Waewthongrak et al., 2014).

142   *B. subtilis* ABS-S14 was isolated from soil collected from citrus groves around the south

143   of Thailand. It was identified by Gram staining, cell shape and the presence of spores, and

144   bio-chemical analysis. The screening test of its antagonistic properties against a fungal

145   colony of *P. digitatum in vitro* was performed prior to use (Leelasuphakul et al., 2008).

146   *2.4. Preparation and purification of CLPs*

147   The *B. subtilis* ABS-S14 strain was grown in LB medium (Waewthongrak et al., 2014),

148   following the method reported (McKeen et al., 1986). A crude extract was prepared from

149   culture-free filtrates obtained after drying in a rotary vacuum evaporator at 65°C. It was

150   weighed and re-dissolved in 80% ethanol, then crude CLP extract was adjusted to a 50 g L^{-1}

151   stock solution (Leelasuphakul et al., 2006). Fengycin, iturin A and surfactin, belonging to the

152   CLP members, were prepared from *B. subtilis* ABS-S14 crude CLP extract using preparative

153   thin-layer chromatography (PTLC) following the reported method (Waewthongrak et al.,

154   2014). They were recovered by ethanol extraction from silica gel on a PTLC plate and further

155   separated using a C18 solid phase extraction (SPE) cartridge (Sep-Pak®, Vac 12 cc (2 g),

156   silica, 15-105 µm, 125 Å pore size, Waters, USA) to increase the purity. A sorbent matrix

157   was eluted by step gradients of acetonitrile in 0.1% trifluoroacetic acid: 40% to 55%, 25% to

158   35% and 60% to 80% for fengycin, iturin A, and surfactin, respectively. The fractions were

159   dried by rotary evaporator and re-dissolved in 80% ethanol.

160   *2.5. Identification of CLPs*

161   Identification of the CLPs was performed by HPLC (Agilent 1200, Agilent Technologies

162   Inc., USA) and matrix-assisted laser desorption ionization time-of-flight (MALDI-TOF) MS

163   (Bruker Daltonic Ultraflex III TOF/TOF, Bruker Daltonics Ltd., Germany) following the

164   previous study (Waewthongrak et al., 2014). The matrix used was α-cyano-4-

165   hydroxycinnamic acid. The bacterial CLPs were detected in the range of molecular ion peaks

166   from m/z 600 to 1,800.

167   *2.6. Inoculation of mandarin fruit*

168   The mandarin oranges were divided into ten treatment groups (five fruit per group with

169   three replicates per group). Artificial wounds were made at two sites on opposite sides of the

170   fruit. Five wounds of a circle of 0.5 cm in diameter and 3 mm in depth were made by

171   puncturing the fruit rind on the equator of the fruit with a sterile needle (Waewthongrak et al.,

172   2014). An aliquot of 20 µL of crude CLP extract (10 g L^{-1}) (Waewthongrak et al., 2015),

173   fengycin (1 g L^{-1}) (Waewthongrak et al., 2014), iturin A (1 g L^{-1}) (Waewthongrak et al.,

174   2014), surfactin (1 g L^{-1}) (Waewthongrak et al., 2014), SA (3.4×10^{-2} g L^{-1}) (Moscoso-

175   Ramírez and Palou, 2013), MeJA (22.2 µL L^{-1}) (Guo et al., 2014), Et (450 µL L^{-1}) (John-

176   Karuppiah and Burns, 2010) in 80% ethanol and *P. digitatum* conidial suspension (10^7 spores

177   L^{-1}) in sterile distilled water was dropped into both wound sites on each fruit, respectively.

178   Consistently, sterile distilled wahter was used as the negative control of *P. digitatum* and

179   ethanol was used as the negative control of exogenous plant hormones (SA, MeJA, and Et)

180   and the extracted products of *B. subtilis* ABS-S14 (CLP extract, fengycin, iturin A, and

181   surfactin). Each treatment was placed in a plastic box containing a cup of water to maintain a

182   high humidity at 25°C and incubated for 24, 48 and 72 h. The appearance of wounds on the

183   treated flavedo tissues (outer colored part of mandarin peel) was observed and photographed

184   daily. The disease incidence was measured from the visible lesion on flavedo tissue by

185   summing the number of fruit with an average lesion $\times 100$ divided by the total number of

186   inoculated wounded fruit (Leelasuphakul et al., 2008; Waewthongrak et al., 2015).

187   *2.7. Extraction of metabolites*

188   The treated flavedo tissue was collected approximately 1 cm away from the wound site.

189   The flavedo tissues in each replicate of the same treatment were pooled and grounded to a

190   fine powder in liquid nitrogen. The metabolites from the fine powder of 15 mg were extracted,

191 based on a method previously reported (Asai et al., 2017), by dissolution in 1 mL of a

192 mixture of methanol/water/chloroform (2.5:1:1 v/v/v), incubation at 40°C for 5 min, and then

193 centrifugation at 14,000 g for 10 min. The supernatant (950 µL) was transferred to a new tube

194 and 400 µL of water was added. The mixture was centrifuged at 14,000 g for 10 min to

195 obtain a polar phase solution. Each sample was transferred to a new tube and stored at -80°C.

196 The workflow of this study for metabolomic analysis is shown in Supplementary Fig. 1.

197 *2.8. Dansylation LC-MS metabolomic profiling*

198 To prepare the samples for dansyl labeling, an individual sample was prepared from 25 µL

199 of the polar phase solution in each replicate. A pooled sample was obtained by mixing small

200 aliquots of all the samples. Methanol was evaporated by a SpeedVac concentrator and 25 µL

201 of water was added just prior to labeling. An individual sample was labeled with ^{12}C-dansyl

202 chloride and the pooled sample was labeled with ^{13}C-dansyl chloride following a reported

203 method (Han et al., 2017). The labeled sample was injected into LC-UV for measuring the

204 total concentration of labeled metabolites for sample amount normalization. For LC-UV, a

205 Waters ACQUITY UPLC system with a photodiode array (PDA) detector operating with a

206 Phenomenex Kinetex C18 column (50 mm × 2.1 mm, 1.7 µm particle size, 100 Å pore size)

207 was used. The total peak areas were detected under 338 nm for the quantification of each

208 sample (Hooton et al., 2016). An equal mole amount of ^{12}C-labeled sample and ^{13}C-labeled

209 pool was mixed. The mixture was then injected into an HPLC system interfaced to an

210 electrospray ionization (ESI) source in a Bruker 9.4 T Apex-Qe Fourier-transform ion

211 cyclotron resonance (FT-ICR) mass spectrometer (Bruker, Billerica, MA). The ESI mass

212 spectra were acquired in the positive ion mode. The setup of FTICR-MS was following a

213 previous report: nitrogen nebulizer gas, 2.3 L min^{-1}; dry gas flow, 7.0 L min^{-1}; dry

214 temperature, 195 °C; capillary voltage, 4200 V; spray shield, 3700 V; acquisition size, 256 k;

215 mass scan range, *m*/z 200 - 1000; ion accumulation time, 1 s; TOF (AQS), 0.007 s; DC

216 extract bias, 0.7 V (Peng et al., 2014). The HPLC flow rate used was 180 µL min⁻¹ and the

217 sample injection volume was 13 µL. The samples were randomly injected in no particular

218 order. Quality control (QC) sample (^{12}C-/^{13}C-labeled pool) was injected every ten sample-

219 runs.

220 *2.9. Data processing*

221 To analyze the ^{12}C-/^{13}C-peak pairs from each LC-MS run, the IsoMS, IsoMS-Align, Zero-

222 fill and IsoMS-Quant programs were used. Metabolites was identified using the DnsID

223 standards library for positive metabolite identification (Huan et al., 2015). A search for

224 putative metabolite identification was performed by MyCompoundID MS software (Huan et

225 al., 2015), against the Human Metabolome Database (HMDB) library and the Evidence-based

226 Metabolome Library (EML) database following the methods described in previous reports

227 (Han et al., 2017; Huan et al., 2015; Shen et al., 2016).

228 *2.10. Statistical analysis*

229 MetaboAnalyst 4.0 was used for principal components analysis (PCA) and pathway

230 analysis of the LC−MS data (Chong et al., 2018). Microsoft Excel was used to calculate the

231 fold change and p-value between groups. Venn diagram was built using in-house R program.

232 Volcano plots (binary comparison) were performed using OriginPro 8.0 (OriginLab). The q-

233 value, multiple-testing-corrected p-value, was calculated using R and BioConductor

234 (www.bioconductor.org). A statistical test of variance of differences (ANOVA) was

235 performed for the data sets of disease incidence and the significant differences in mean values

236 were determined with the Tukey's range test ($p \leq 0.05$).

237 **3. Results**

238   CLPs of *B. subtilis* ABS-S14 are composed of three main compounds, fengycin, iturin A

239   and surfactin (Waewthongrak et al., 2014). To test their effects on wound appearance

240   development, these compounds were firstly separated with C18-SPE and verified with HPLC

241   and MALDI-TOF MS. Fengycin, iturin A and surfactin were recovered from the bacterial

242   CLP extract after eluted from the C18 SPE cartridge at the intervals of 19-32, 5-18 and 41-57

243   min of retention time (Supplementary Fig. 2). The MALDI-TOF MS spectra of the extracts at

244   three intervals of *m/z* values in the ranges of 1,449.74-1,547.82, 1,058.61-1,110.60 and

245   1,044.61-1,074.62 were found to match with those of the commercial standards (Sigma-

246   Aldrich, USA) (Supplementary Fig. 3).

247   *3.1. Effect of plant tissue treatments on wound appearances*

248   The progression of various treatments on wound appearance development on flavedo

249   tissues showed distinguished patterns of damage change (Fig. 1). In the *P. digitatum* infected

250   flavedo treatment, occurrence of watery spots was only observed on the wound sites of the

251   pathogen infected flavedo tissues when compared with the negative control (sterile distilled

252   water) at 72 h post-treatment. Treatments of exogenous plant hormones showed a similar

253   pattern of wound appearance of brown-damaged spots on flavedo tissues when compared

254   with the negative control (ethanol) from the first day to the end of treatment. On the contrary,

255   the treatments with the extracted *B. subtilis* ABS-S14 products (CLP extracts, fengycin, iturin

256   A and surfactin) showed much less brown-damaged spot and revealed statistically significant

257   reduction of disease incidence on flavedo tissues than plant hormone and ethanol treatments

258   (Supplementary Fig. 4).

259   *3.2. Submetabolome profiling and metabolite identification*

260   Metabolites in the treated flavedo tissues of the mandarin fruit were profiled using [12]C-

261   /^{13}C-dansylation LC-MS analysis. A total of 4,914±111 peak pairs or metabolites were

262   detected in the duplicate analysis of 90 flavedo samples. Note that IsoMS filtered out all

263   redundant peak pairs of the same metabolite such as adducts or dimers and then retained only

264   one peak pair for one labeled metabolite. Thus, the number of peak pairs reflects the number

265   of metabolites detected. Among these detected metabolites, 77 metabolites were positively

266   identified using a dansyl standard library search based on accurate mass and retention time

267   matches (Supplementary Table 1) (Huan et al., 2015). In addition, 666 and 2,769 peak pairs

268   were mass-matched to metabolites in the HMDB library and the EML library, respectively

269   (Supplementary Tables 2 and 3) (Huan et al., 2015). These results indicated that dansylation

270   LC-MS could be used to detect a large number of amine- and phenol-containing metabolites.

271   More importantly, the metabolome composition of the flavedo samples appeared to be very

272   complex and the detected 77 positively identified metabolites plus many more putatively

273   matched metabolite covers a wide range of metabolic pathways, which will be discussed in

274   the section of pathway analysis.

275   *3.3. Plant metabolome profiles and comparison*

276   From the data set of 180 LC-MS runs of 90 samples, we used statistical tools to analyze

277   the metabolome differences among different groups of samples. PCA showed distinct

278   separations from tested samples using different treatments of various substances and from

279   samples of different time points as well as the 19 QC runs (Fig. 2A). The metabolome data

280   could be separated into four major groups plus the QC group. Very tight clustering of the QC

281   runs indicated the high reproducibility of the analysis, which was not surprising because the

282   ^{13}C-labeled pool was used as the internal control of all the ^{12}C-labeled samples in our analysis.

283   Using a heavy-isotope labeled internal control greatly reduced the ion suppression and matrix

284   effects as well as compensated for instrument sensitivity drift, if any, during the sample runs.

285   In Fig. 2A, samples from different agents applied at different time points are labeled with

286   different colors. Samples from the same agent at the same time point such as the samples in

287   iturin A treatment at 24 h post-treatment are categorized into the same group. Fig. 2B shows

288   the four-color PCA plot of the samples with various treatments at all time points. The

289   samples with sterile distilled water and ethanol were clustered together (green) and defined as

290   the control group for wound stress. The sample groups colored in light blue, blue, and red

291   represented the treatment groups with *P. digitatum*, exogenous plant hormones, and extracts

292   of *B. subtilis* ABS-S14 (i.e., CLP extracts containing fengycin, iturin A, and surfactin and the

293   separated fengycin, iturin A and surfactin compounds), respectively.

294   The labeled samples in the groups of control (green color) and exogenous plant hormones

295   (blue color) at all time points had sub-groups in their treatments as shown in the red circle in

296   Fig. 2B. The sub-groups in the red circle of Fig. 2B were identified in different color-labeled

297   samples as shown in red circle of Fig. 2C. Based on the time point analysis of each treatment

298   (Fig. 2C), clustering of the samples was detected in tissues treated with *P. digitatum* (black

299   color) and CLPs (red color) at every time point. The similar pattern of clustering together at

300   24 and 48 h post-treatment from the treatment group of exogenous plant hormones and the

301   control (yellow and green colored groups, respectively) was showed in the PCA plot of the

302   metabolome data (Fig. 2C); however, the samples detected at 72 h post-treatment clustered

303   differently. Fig. 2C shows that the treatment of ethephon at 24 h post-treatment deviated from

304   the samples at 48 and 72 h post-treatment.

305   Supplementary Fig. 5 shows the Venn diagram of the peak pair or metabolite numbers

306   detected from the four major treatment groups. There were 3,957 metabolites commonly

307   detected in the four major groups. Only a very small fraction of the metabolites were

308   uniquely detected in each group (i.e., 57, 24, 72, and 66 unique metabolites were found in the

309   treatments of CLPs, *P. digitatum*, exogenous plant hormone, and control, respectively). To

310   determine the metabolic changes, we further analyzed the data using binary comparisons of

311   different groups. The resulting volcano plots indicated the metabolic changes of the fruit peel

312   samples after being exposed to fungal pathogen, exogenous plant hormones, and *B. subtilis*

313   ABS-S14 CLPs, respectively, as compared to their corresponding control group (Fig. 3). In

314   the preparation of the *P. digitatum* spore suspension, sterile distilled water was used, whereas

315   ethanol was used for the solutions of exogenous plant hormone and CLPs. Therefore, the

316   effect of water or ethanol was discounted using binary comparison analysis of the

317   submetabolome in the treated group vs. its corresponding control (i.e., *P. digitatum* treatment

318   vs. water, exogenous plant hormones vs. ethanol, and CLPs vs. ethanol). In addition, any

319   change in metabolite concentration of more than 1.5-fold and a q-value of below 0.05 with

320   associated p-value was considered as being significant.

321   The volcano plot analysis of *P. digitatum* treatment vs. control (Fig. 3A) indicates that out

322   of 4,577 metabolites, 1,061 metabolites were down-regulated (i.e., lower metabolite

323   concentration in the treated samples than that of the control) and 407 metabolites were up-

324   regulated (i.e., higher metabolite concentration in the treated samples). In the group of

325   exogenous plant hormones vs. control (Fig. 3B), out of 4,545 metabolites, only three

326   metabolites were found to be down-regulated and 17 metabolites were up-regulated.

327   Interestingly, in the group of CLPs vs. control (Fig. 3C), out of 4,594 metabolites, 748

328   metabolites were down-regulated and 600 metabolites were up-regulated. Regarding the

329   significantly changed metabolites in the three binary comparisons, the group of CLPs showed

330   the greatest number of up-regulated metabolites. This group also showed the greatest

331   numbers of positively identified metabolites among the tested groups, based on a search in

332   the dansyl standard library (Huan et al., 2015). Noticeably, the treated group of exogenous

333   plant hormones had the minor changes in metabolite regulation whereas the group of fungal

334   infection showed the greatest numbers of down-regulated metabolites.

335   *3.4. Metabolite regulation in plant defense to stress responses*

336   *B. subtilis* CLPs elicited the largest number of metabolite changes in the plant stress

337   responses (Fig. 3), indicating that CLPs are better than exogenous plant hormones in

338   triggering the synthesis of plant defense metabolites. The 77 identified positive metabolites

339   were exported for pathway analysis using the MetaboAnalyst 4.0 software based on the

340   *Arabidopsis thaliana* database since no citrus plant database was available (Chong et al.,

341   2018). Totally 39 pathways matched to the 77 positively identified metabolites. As shown in

342   Fig. 4, each pathway contained an impact and a p-value according to numbers of 'hits'

343   recorded and the significance factors of the detected metabolites. The highest pathway impact

344   and statistical significance was located on the top right corner (Fig. 4). The metabolism of

345   glycine, serine and threonine, which plays an important role in postharvest stress response,

346   had the highest pathway impact and statistical significance. The activation of some other

347   metabolites was also detected in pathways that play a role in postharvest stress responses,

348   including alanine, aspartate and glutamate metabolism, beta alanine metabolism, isoquinoline

349   alkaloid biosynthesis, tyrosine metabolism, pantothenate and CoA biosynthesis, carbon

350   fixation in photosynthetic organisms, aminoacyl-tRNA biosynthesis, phenylpropanoid

351   biosynthesis, pyrimidine metabolism, glutathione metabolism and lysine biosynthesis (Fig.

352   4).

353   Since the glycine, serine and threonine pathway and the tyrosine pathway contain vital

354   amino acids (i.e. tryptophan and tyrosine) which are important for synthesis of secondary

355   metabolites (i.e. serotonin and tyramine) leading to plant defense, these two pathways were

356   further analyzed. The metabolites yet to be identified were shown in light blue boxes, the

357   positively identified metabolites were highlighted in green, and the putatively identified

358   metabolites were highlighted in orange (Figs. 5 and 6). The box plot of each positively or

359   putatively identified metabolite in the pathway was included to show the significant level

360 changes compared to the control group (Figs. 5 and 6). As shown in Fig. 5, six of the 77

361 identified metabolites involve in the metabolism of glycine, serine and threonine, and four

362 metabolites belong to the tryptophan metabolism. In terms of the tyrosine pathway, two

363 positively identified metabolites, i.e., tyrosine and tyramine (in green) and four putatively

364 identified metabolites (in orange) were found (Fig. 6).

365   The crude CLP extract and each CLP obtained from *B. subtilis* ABS-S14 were found to be

366 able to trigger the synthesis of secondary metabolites like serotonin (Fig. 7A) and 5-hydroxy-

367 *N*-methyltryptamine (Fig. 7B) in flavedo tissues. Accordingly, the box plot of tyrosine

368 concentration in the CLPs treated group showed a lower level than those found in the other

369 agent treated groups (Fig. 7C). Tyrosine had been immediately changed to tyramine as

370 validated by the box plot of Tyramine/Tyrosine (Fig. 7D). Thus, some agents in the CLPs

371 group such as crude CLP extract and fengycin treatments were able to highly activate

372 tyramine production, compared to the other groups (Fig. 7E). The comparative metabolic

373 changes of fungal infection, including the treatments of exogenous plant hormones and CLPs

374 on the production of primary and secondary metabolites in tryptophan and tyrosine pathways

375 (Fig. 7), provided evidence that *P. digitatum* had only a minor effect on those metabolites in

376 mandarin fruit. In the same manner, the effects of exogenous plant hormones were similar to

377 fungal infection on those metabolites with the exception that the treatments of SA, MeJA and

378 Et and their controls were able to elicit greater accumulations of tyrosine than the treatment

379 of CLPs and the fungal pathogen in mandarin fruit.

380 **4. Discussion**

381   Metabolomics studies of plant responses to various kinds of stresses have been carried out

382 in order to provide a better understanding of metabolic changes associated with the

383 enhancement of plant resistance, especially postharvest treatments of citrus fruit (Asai et al.,

384 2017; Servillo et al., 2013). For instance, differential accumulation of significant proteins and

385 metabolites in Satsuma mandarin after heat treatment revealed reactive oxygen species and

386 lignin that played roles in induced fruit resistance to pathogen (Yun et al, 2013). The

387 application of exogenous phytohormones such as SA and MeJA also affected the metabolic

388 changes in citrus leaves during defense response (Asai et al., 2017). The expression of plant

389 defensive genes inducing by *B. subtilis* CLPs was demonstrated in citrus fruit at

390 transcriptional levels (Waewthongrak et al., 2014). However, the action of *B. subtilis* CLPs

391 on stimulating metabolic changes in defense mechanism in postharvest mandarin fruit was

392 still unclear.

393   In this study, metabolomics was used to differentiate effects of agents including *B. subtilis*

394 CLPs, exogenous plant hormones, and *P. digitatum* on the metabolic changes of postharvest

395 mandarin fruit under wound stress. Mandarin fruit treated with *B. subtilis* CLPs showed

396 significant better healing of the wound sites than *P. digitatum* and exogenous plant hormones

397 (Fig. 1), indicating *B. subtilis* CLPs treatment may trigger a more effective defense

398 mechanism under stress to protect the fruit. We subsequently applied dansylation LC-MS to

399 examine the metabolic differences of the amine/phenol submetabolome in the wound tissues

400 to study the affected metabolic pathways in the host plant, with the focus on defense

401 responses.

402   Consistent with the healing observation (Fig. 1), these agents had different levels of

403 capability to trigger metabolite accumulations in the treated flavedo tissues. A close

404 relationship between the exogenous plant hormones and wounding effects on metabolite

405 induction was observed in their treatments at the early time point (24 h post-treatment) and

406 the late time points (48 and 72 h post-treatment) (Fig. 2C). The exogenous plant hormones

407 and wounding effects might share a common pathway in their metabolite regulation function

408 in mandarin peel (Fig. 2B and 2C). Our results were consistent with a previous study in citrus

409   leaves, which demonstrated that both tryptophan and serine were highly sensitive to stress

410   treatments (Asai et al., 2017). Moreover, the wounding and MeJA treatment showed that

411   amino acid abundances such as tryptophan were up-regulated with serine being down-

412   regulated, indicating that the *de novo* synthesis of tryptophan occurred due to the conversion

413   of serine and indole (Asai et al., 2017).

414   The metabolomic analysis showed large metabolic changes in the wound tissues treated

415   with the *B. subtilis* CLP extract and its major bioactive compounds fengycin, iturin A and

416   surfactin (Fig. 3C). These agents appeared to be able to powerfully trigger metabolic changes

417   in the flavedo tissues in responses to wound stress during the postharvest period. This

418   metabolomic finding was consistent with a previous study which demonstrated that *B. subtilis*

419   ABS-S14 CLPs elicited the expression of defense–related genes and the accumulation of

420   enzymes in the induced systemic resistance system (Waewthongrak et al., 2014). Our work

421   also indicated that the metabolites specifically induced by CLP extracts and an individual

422   agent in *B. subtilis* CLPs were involved in twelve major pathways: the glycine, serine and

423   threonine metabolism and the tyrosine metabolism (Fig. 4).

424   Glycine, serine and threonine metabolism may play significant physiological roles in some

425   aspects of stress response in mandarin flavedo tissues induced by bacterial CLPs. On the

426   other hand, phenylalanine, tryptophan, and tyrosine were reported to accumulate after

427   wounding and MeJA and SA treatments (Asai et al., 2017), which were consistent with our

428   finding that the treatments of exogenous plant hormones after wounding increased the

429   abundance of tryptophan and tyrosine. Tryptophan and tyrosine metabolisms might be

430   involved in key regulation in response to stresses. The overall functional categories of each

431   amino acid and their derivatives of glycine, serine and threonine metabolism found to be

432   significant in this metabolomic study (Fig. 5). Specifically, aspartic acid not only acts as the

433   precursor for the synthesis of asparagine which mediates nitrogen transport and storage in

434   plants, but also serves as the precursor for generating aspartate-derived amino acids which are

435   located in leaves, seeds and roots (Azevedo et al., 2006). Moreover, homoserine can activate

436   plant growth (Palmer et al., 2014) and threonine, a substrate of threonine deaminase in α-

437   ketobutyrate and ammonia biosynthesis, is involved in plant defense (Gonzales-Vigil et al.,

438   2011). In addition, serine was one of the most important amino acids involving in the

439   photorespiratory glycolate pathway for plant metabolism and development (Ros et al., 2014),

440   glycine is involved in plant development via the root system (Domínguez-May et al., 2013),

441   and tryptophan is a precursor for generating secondary metabolites in plant immunity (Dixon

442   and Paiva, 1995; Servillo et al., 2013).

443   Previous studies also showed that tryptophan has important role in plant defense (Ishihara

444   et al., 2008; Servillo et al., 2013) and acts as the precursor of serotonin (Ishihara et al., 2008).

445   Surprisingly, serotonin and its derivative 5-hydroxy-*N*-methyltryptamine were significantly

446   up-regulated in the treatment group of *B. subtilis* CLPs (Fig. 7A and B). The bacterial CLPs

447   treatment could activate the serotonin and 5-hydroxy-*N*-methyltryptamine synthesis at a

448   higher level than the other treatments at all time-points (Fig. 7A and B). Serotonin is involved

449   in the plant defense mechanism (Servillo et al., 2015). Specifically, it serves as a substrate of

450   peroxidase to create polymers like lignin that functions as a physical barrier to inhibit the

451   spread of the pathogen infection (Ishihara et al., 2008). Even though the direct function of 5-

452   hydroxy-*N*-methyltryptamine in plant defense is still unclear, this metabolite may act as a

453   precursor for glucosylated serotonin derivatives which can produce toxic aglycones to attack

454   the pathogen via glycosidase activity (Servillo et al., 2015).

455   The present study also found that tyrosine abundance was down-regulated in *B. subtilis*

456   CLP treatment group since it was acting as a precursor of tyramine (Fig. 7D). Therefore, the

457   role of tyramine was confirmed as the precursor of tyramine derivatives that are involved in

458   the pathways of the plant defense mechanism (Servillo et al., 2017). Moreover, tyramine

459   derivatives were coproduced with specialized defensive secondary metabolites, such as toxic

460   substances produced by the plant, to attack a pathogen in response to an infection (Servillo et

461   al., 2014). The large abundance of tyrosine induced by exogenous plant hormones might

462   serve as a precursor to produce downstream substances in the pathway (Fig. 6), but it did not

463   influence tyramine accumulation (Fig. 7E). In addition, unlike *B. subtilis* CLPs, *P. digitatum*

464   and exogenous plant hormones did not stimulate the synthesis of serotonin, 5-hydroxy-*N*-

465   metyltryptamine, tyrosine or tyramine in the metabolism of tryptophan and tyrosine in

466   mandarin fruits under wound stress.

467   Extracts of *B. subtilis* ABS-S14, exogenous phytohormones, and *P. digitatum* infection

468   affected the accumulation of primary and secondary metabolites to stress responses in

469   mandarin fruit during storage period. Each amino acid can be the precursor to produce a

470   number of metabolites. The function of each metabolite could be affected in many pathways

471   (Dinkeloo et al., 2018). The altered levels of some amino acids could impact the systems of

472   host plant such as in defensive pathway (Zeier, 2013), e.g., serotonin could be induced by the

473   application of *B. subtilis* ABS-S14 CLPs, but not by *P. digitatum*. To increase or decrease

474   the production of amino acids, stress is one of the factors which can trigger the mechanisms

475   of host plant (Tunsagool et al., 2019). Thus, amino acids are the most changed pathway of

476   different treatments. Moreover, the changes of metabolites on flavedo tissues by these agents

477   resulted in healing ability of wound sites. The greater effect of wound healing was observed

478   in the group of *B. subtilis* ABS-S14 CLP treatments than those of other agents. *Bacillus* CLPs

479   employed the metabolisms of glycine, serine and threonine, tryptophan, and tyrosine to

480   increase the production of secondary metabolites such as serotonin and tyramine during

481   stresses, leading to the induction of plant immunity. According to the factors of green mold

482   infection in mandarin fruit, wound sites on mandarin peel were the main factor for *P.*

483   *digitatum* growth. Healing ability by the effect of preventive applications of *B. subtilis* ABS-

484   S14 CLPs could reduce the chance of green mold infection in mandarin fruit. Taking together,

485   the healing outcome observed, in combination with the understanding of metabolic changes

486   in flavedo tissues by the treatments of *B. subtilis* ABS-S14 CLPs, suggested this extract as an

487   alternative agent for the protection of mandarin fruit against green mold pathogen invasion

488   during postharvest storage.

489   **5. Conclusions**

490   In summary, application of extracted CLP compounds from *B. subtilis* ABS-S14 showed

491   the greatest effect on healing ability of wound sites in mandarin fruit than exogenous plant

492   hormones, indicating that they are promising biological regents in prevention of green mold

493   rot on mandarin fruit during postharvest period. The metabolome differences of wound

494   tissues treated with different agents were profiled with extensive metabolomic analysis with

495   dansylation LC-MS and the results showed that the applied agents played a role in regulation

496   of primary and secondary metabolites during storage period. The metabolisms of glycine,

497   serine and threonine, tryptophan, and tyrosine were found to be the important signal

498   transductions of the action of *B. subtilis* CLPs in stress responses. An increase of secondary

499   metabolite accumulation such as serotonin and tyramine in CLP treatments involved the

500   elicitation of defensive system of plant resistance.

501

515

516   **Appendix A. Supplementary data**

517   Supplementary materials are included.

518

519   **References**

520   Asai, T., Matsukawa, T., Kajiyama, S., 2017. Metabolomic analysis of primary metabolites in

521   citrus leaf during defense responses. J. Biosci. Bioeng. 123, 376-381.

522   Azevedo, R.A., Lancien, M., Lea, P.J., 2006. The aspartic acid metabolic pathway, an

523   exciting and essential pathway in plants. Amino Acids 30, 143-162.

524   Ballester, A.R., Teresa Lafuente, M., Gonzalez-Candelas, L., 2013. Citrus phenylpropanoids

525   and defence against pathogens. Part II: gene expression and metabolite accumulation in

526   the response of fruits to *Penicillium digitatum* infection. Food Chem. 136, 285-291.

527   Chong, J., Soufan, O., Li, C., Caraus, I., Li, S., Bourque, G., Wishart, D.S., Xia, J., 2018.

528   MetaboAnalyst 4.0: towards more transparent and integrative metabolomics analysis.

529   Nucleic Acids Res. 46, W486-W494.

530 Dinkeloo, K., Boyd, S., Pilot, G., 2018. Update on amino acid transporter functions and on

531   possible amino acid sensing mechanisms in plants. Semin. Cell Dev. Biol. 74, 105-113.

532 Dixon, R.A., Paiva, N.L., 1995. Stress-induced phenylpropanoid metabolism. Plant Cell 7,

533   1085-1097.

534 Domínguez-May, Á.V., Carrillo-Pech, M., Barredo-Pool, F.A., Martínez-Estévez, M., Us-

535   Camas, R.Y., Moreno-Valenzuela, O.A., Echevarría-Machado, I., 2013. A novel effect

536   for glycine on root system growth of habanero pepper. J. Amer. Soc. Hort. Sci. 138, 433-

537   442.

538 Eckert, J.W., 1978. Post-harvest diseases of citrus fruits. Outlook on Agriculture 9, 225-232.

539 Gonzales-Vigil, E., Bianchetti, C.M., Phillips, G.N., Jr., Howe, G.A., 2011. Adaptive

540   evolution of threonine deaminase in plant defense against insect herbivores. Proc. Natl.

541   Acad. Sci. U.S.A. 108, 5897-5902.

542 Guo, J., Fang, W., Lu, H., Zhu, R., Lu, L., Zheng, X., Yu, T., 2014. Inhibition of green mold

543   disease in mandarins by preventive applications of methyl jasmonate and antagonistic

544   yeast *Cryptococcus laurentii*. Postharvest Biol. Technol. 88, 72-78.

545 Guo, K., Li, L., 2009. Differential ^{12}C-/^{13}C-isotope dansylation labeling and fast liquid

546   chromatography/mass spectrometry for absolute and relative quantification of the

547   metabolome. Anal. Chem. 81, 3919-3932.

548 Hall, R., Beale, M., Fiehn, O., Hardy, N., Sumner, L., Bino, R., 2002. Plant metabolomics:

549   the missing link in functional genomics strategies. Plant Cell 14, 1437-1440.

550 Han, W., Sapkota, S., Camicioli, R., Dixon, R.A., Li, L., 2017. Profiling novel metabolic

551   biomarkers for Parkinson's disease using in-depth metabolomic analysis. Mov. Disord.

552   32, 1720-1728.

553   Hooton, K., Han, W., Li, L., 2016. Comprehensive and quantitative profiling of the human

554   sweat submetabolome using high-performance chemical isotope labeling LC-MS. Anal.

555   Chem. 88, 7378-7386.

556   Huan, T., Wu, Y., Tang, C., Lin, G., Li, L., 2015. DnsID in MyCompoundID for rapid

557   identification of dansylated amine- and phenol-containing metabolites in LC-MS-based

558   metabolomics. Anal. Chem. 87, 9838-9845.

559   Ishihara, A., Hashimoto, Y., Tanaka, C., Dubouzet, J.G., Nakao, T., Matsuda, F., Nishioka, T.,

560   Miyagawa, H., Wakasa, K., 2008. The tryptophan pathway is involved in the defense

561   responses of rice against pathogenic infection via serotonin production. Plant J. 54, 481-

562   495.

563   John-Karuppiah, K.-J., Burns, J.K., 2010. Expression of ethylene biosynthesis and signaling

564   genes during differential abscission responses of sweet orange leaves and mature fruit. J.

565   Amer. Soc. Hort. Sci. 135, 456-464.

566   Leelasuphakul, W., Hemmanee, P., Chuenchitt, S., 2008. Growth inhibitory properties of

567   *Bacillus subtilis* strains and their metabolites against the green mold pathogen

568   (*Penicillium digitatum* Sacc.) of citrus fruit. Postharvest Biol. Technol. 48, 113-121.

569   Leelasuphakul, W., Sivanunsakul, P., Phongpaichit, S., 2006. Purification, characterization

570   and synergistic activity of β-1,3-glucanase and antibiotic extract from an antagonistic

571   *Bacillus subtilis* NSRS 89-24 against rice blast and sheath blight. Enzyme Microb.

572   Technol. 38, 990-997.

573   Luo, X., Zhao, S., Huan, T., Sun, D., Friis, R.M., Schultz, M.C., Li, L., 2016. High-

574   performance chemical isotope labeling liquid chromatography-mass spectrometry for

575   profiling the metabolomic reprogramming elicited by ammonium limitation in yeast. J.

576   Proteome Res. 15, 1602-1612.

577   McKeen, C.D., Reilly, C.C., Pusey, P.L., 1986. Production and partial characterization of

578   antifungal substances antagonistic to *Monilinia fructicola* from *Bacillus subtilis*.

579   Phytopathology 76, 136-139.

580   Moscoso-Ramírez, P.A., Palou, L., 2013. Evaluation of postharvest treatments with chemical

581   resistance inducers to control green and blue molds on orange fruit. Postharvest Biol.

582   Technol. 85, 132-135.

583   Ongena, M., Jacques, P., 2008. *Bacillus* lipopeptides: versatile weapons for plant disease

584   biocontrol. Trends Microbiol. 16, 115-125.

585   Palmer, A.G., Senechal, A.C., Mukherjee, A., Ane, J.M., Blackwell, H.E., 2014. Plant

586   responses to bacterial N-acyl L-homoserine lactones are dependent on enzymatic

587   degradation to L-homoserine. ACS Chem. Biol. 9, 1834-1845.

588   Palou, L., Smilanick, J., Droby, S., 2008. Alternatives to conventional fungicides for the

589   control of citrus postharvest green and blue molds. Stewart Postharvest Rev. 4, 1–16.

590   Peng, J., Guo, K., Xia, J., Zhou, J., Yang, J., Westaway, D., Wishart, D.S., Li, L., 2014.

591   Development of isotope labeling liquid chromatography mass spectrometry for mouse

592   urine metabolomics: quantitative metabolomic study of transgenic mice related to

593   Alzheimer's disease. J. Proteome Res. 13, 4457-4469.

594   Price, N.P., Rooney, A.P., Swezey, J.L., Perry, E., Cohan, F.M., 2007. Mass spectrometric

595   analysis of lipopeptides from *Bacillus* strains isolated from diverse geographical

596   locations. FEMS Microbiol. Lett. 271, 83-89.

597   Ros, R., Munoz-Bertomeu, J., Krueger, S., 2014. Serine in plants: biosynthesis, metabolism,

598   and functions. Trends Plant Sci. 19, 564-569.

599   Rosier, A., Medeiros, F.H.V., Bais, H.P., 2018. Defining plant growth promoting

600   rhizobacteria molecular and biochemical networks in beneficial plant-microbe

601   interactions. Plant Soil 428, 35-55.

602   Sampaio, B.L., Edrada-Ebel, R., Da Costa, F.B., 2016. Effect of the environment on the

603   secondary metabolic profile of *Tithonia diversifolia*: a model for environmental

604   metabolomics of plants. Sci Rep 6, 29265.

605   Servillo, L., Castaldo, D., Giovane, A., Casale, R., D'Onofrio, N., Cautela, D., Balestrieri,

606   M.L., 2017. Tyramine pathways in citrus plant defense: Glycoconjugates of tyramine

607   and its N-methylated derivatives. J. Agric. Food Chem. 65, 892-899.

608   Servillo, L., Giovane, A., Balestrieri, M.L., Casale, R., Cautela, D., Castaldo, D., 2013.

609   *Citrus* genus plants contain N-methylated tryptamine derivatives and their 5-

610   hydroxylated forms. J. Agric. Food Chem. 61, 5156-5162.

611   Servillo, L., Giovane, A., Casale, R., D'Onofrio, N., Ferrari, G., Cautela, D., Balestrieri, M.L.,

612   Castaldo, D., 2015. Serotonin 5-*O*-*β*-glucoside and its N-methylated forms in *Citrus*

613   genus plants. J. Agric. Food Chem. 63, 4220-4227.

614   Servillo, L., Giovane, A., D'Onofrio, N., Casale, R., Cautela, D., Ferrari, G., Balestrieri, M.L.,

615   Castaldo, D., 2014. N-methylated derivatives of tyramine in *Citrus* genus plants:

616   identification of *N*,*N*,*N*-trimethyltyramine (candicine). J. Agric. Food Chem. 62, 2679-

617   2684.

618   Shen, W., Han, W., Li, Y., Meng, Z., Cai, L., Li, L., 2016. Development of chemical isotope

619   labeling liquid chromatography mass spectrometry for silkworm hemolymph

620   metabolomics. Anal. Chim. Acta. 942, 1-11.

621   Talibi, I., Boubaker, H., Boudyach, E.H., Ait Ben Aoumar, A., 2014. Alternative methods for

622   the control of postharvest citrus diseases. J. Appl. Microbiol. 117, 1-17.

623   Tugizimana, F., Piater, L., Dubery, I., 2013. Plant metabolomics: A new frontier in

624   phytochemical analysis. S. Afr. J. Sci. 109, 1-11.

625   Tunsagool, P., Jutidamrongphan, W., Phaonakrop, N., Jaresitthikunchai, J., Roytrakul, S.,

626   Leelasuphakul, W., 2019. Insights into stress responses in mandarins triggered by

627   *Bacillus subtilis* cyclic lipopeptides and exogenous plant hormones upon *Penicillium*

628   *digitatum* infection. Plant Cell Rep. 38, 559-575.

629   Vlot, A.C., Dempsey, D.A., Klessig, D.F., 2009. Salicylic acid, a multifaceted hormone to

630   combat disease. Annu. Rev. Phytopathol 47, 177-206.

631   Waewthongrak, W., Leelasuphakul, W., McCollum, G., 2014. Cyclic lipopeptides from

632   *Bacillus subtilis* ABS-S14 elicit defense-related gene expression in citrus fruit. PLoS

633   ONE 9, e109386.

634   Waewthongrak, W., Pisuchpen, S., Leelasuphakul, W., 2015. Effect of *Bacillus subtilis* and

635   chitosan applications on green mold (*Penicilium digitatum* Sacc.) decay in citrus fruit.

636   Postharvest Biol. Technol. 99, 44-49.

637   Yun, Z., Gao, H., Liu, P., Liu, S., Luo, T., Jin, S., Xu, Q., Xu, J., Cheng, Y., Deng, X., 2013.

638   Comparative proteomic and metabolomic profiling of citrus fruit with enhancement of

639   disease resistance by postharvest heat treatment. BMC Plant Biol. 13, 44.

640   Zeier, J., 2013. New insights into the regulation of plant immunity by amino acid metabolic

641   pathways. Plant Cell Environ. 36, 2085-2103.

642   Zhou, Y., Ma, J., Xie, J., Deng, L., Yao, S., Zeng, K., 2018. Transcriptomic and biochemical

643   analysis of highlighted induction of phenylpropanoid pathway metabolism of citrus fruit

644   in response to salicylic acid, *Pichia membranaefaciens* and oligochitosan. Postharvest

645   Biol. Technol.142, 81-92.

646

647

648 **Figure captions**

649 **Fig. 1.** Wound appearance in each treatment at 24, 48, and 72 h post-treatment.

650 **Fig. 2.** PCA plots of the metabolomic data obtained from different groups of samples

651 including QC samples. (A) Color-coded groups according to the treatments at all

652 time points and the QC group. (B) Color-coded groups according to the treatment

653 times of 24, 48 and 72 h from four major groups of treatments. (C) Color-coded sub-

654 groups within the control and exogenous plant hormone groups. W, sterile distilled

655 water; E, ethanol; Pd, *Penicillium digitatum*; SA, salicylic acid; MeJA, methyl

656 jasmonate; Et, ethephon; CE, crude CLP extract; F, fengycin; I, iturin A; S, surfactin;

657 CLPs, cyclic lipopeptide group; PH, exogenous plant hormones; 24, 24 h post-

658 treatment; 48, 48 h post-treatment; 72, 72 h post-treatment.

659 **Fig. 3.** Volcano plots of binary comparisons of metabolites in treatment vs. control. (A)

660 *Penicillium digitatum* treatment group vs. water group. (B) Exogenous plant

661 hormone treatment group vs. ethanol group. (C) CLP treatment group vs. ethanol

662 group. The significant metabolites are shown in red or blue with fold change > 1.5

663 and q=value <0.05 with corresponding P <0.134 in (A), P <0.014 in (B) and P

664 <0.216 in (C).

665 **Fig. 4.** Overview of metabolic pathway analysis relating to stress responses.

666 **Fig. 5.** Metabolic pathway of glycine, serine and threonine metabolism including tryptophan

667 metabolism. The metabolite in green box represents the positive ID, orange box

668 represents the putative ID, and blue box represents no ID, and the box plots of

669 identified metabolites are displayed beside the corresponding metabolites. E, ethanol;

670 CLPs, cyclic lipopeptide group.

671 **Fig. 6.** Metabolic pathway of tyrosine metabolism. The metabolite in green box represents

672 the positive ID, orange box represents the putative ID, and blue box represents no ID,

673   and the box plots of identified metabolites are displayed beside the corresponding

674   metabolites. E, ethanol; CLPs, cyclic lipopeptide group.

675 **Fig. 7.** Box plots of positively identified metabolites related to plant defense pathway: (A)

676   serotonin, (B) 5-hydroxy-*N*-methyltryptamine, (C) tyrosine, (D) tyramine/tyrosine,

677   and (E) tyramine. W, sterile distilled water; E, ethanol; Pd, *Penicillium digitatum*;

678   SA, salicylic acid; MeJA, methyl jasmonate; Et, ethephon; CE, crude CLP extract; F,

679   fengycin; I, iturin A; S, surfactin. Vertical bars represent standard errors of the mean

680   value of six trials.
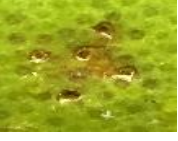
Treatments	24 h	48 h	72 h
Sterile distilled water			
Penicillium digitatum			
Ethanol			
Salicylic acid			
Methyl jasmonate			
Ethephon			
CLP extract			
Fengycin			
Iturin A			
Surfactin			

Figure 1
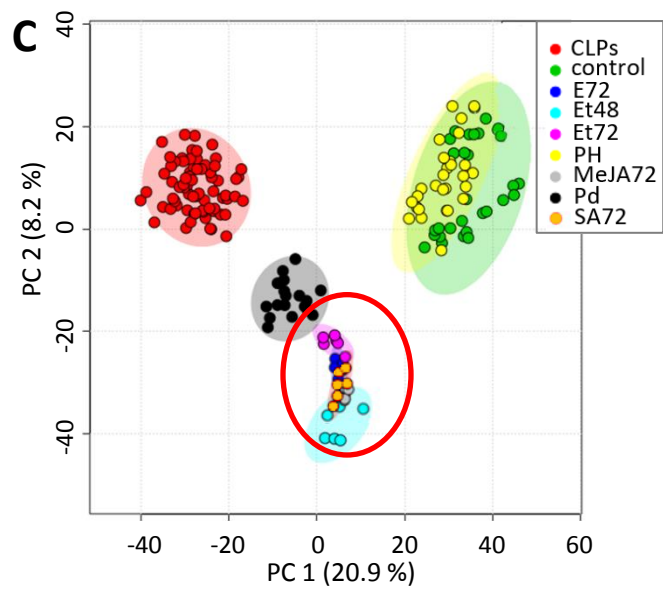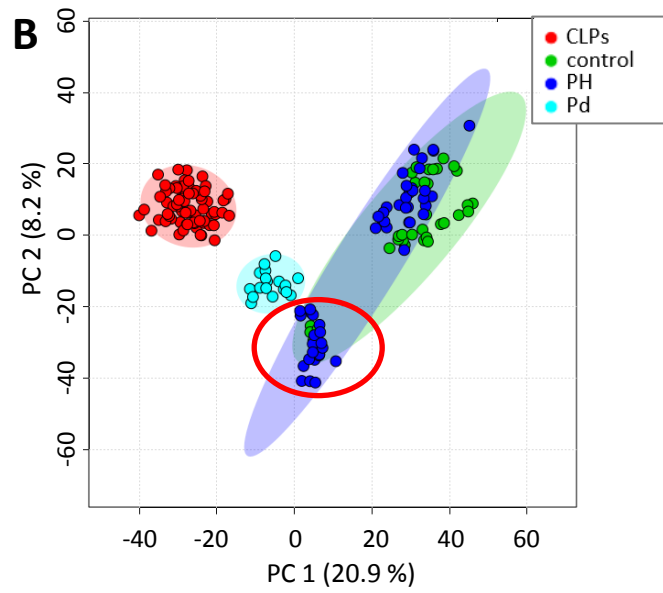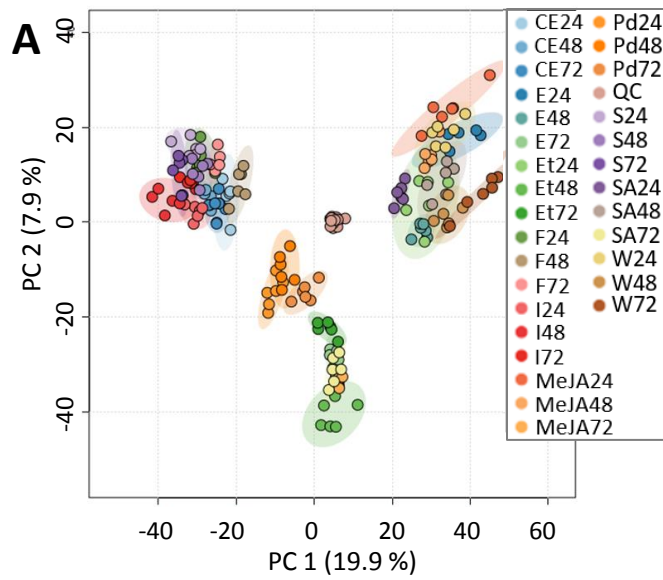
Figure 2
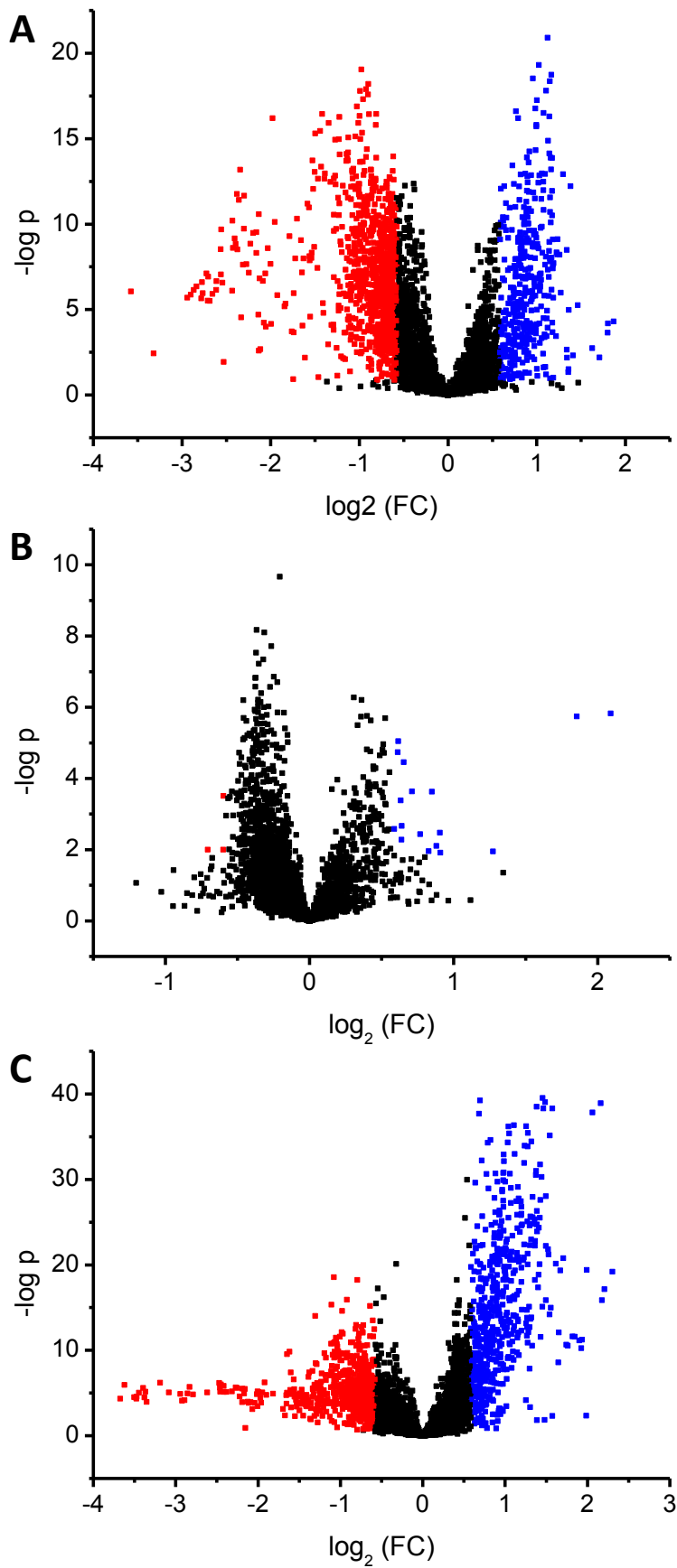
Figure 3
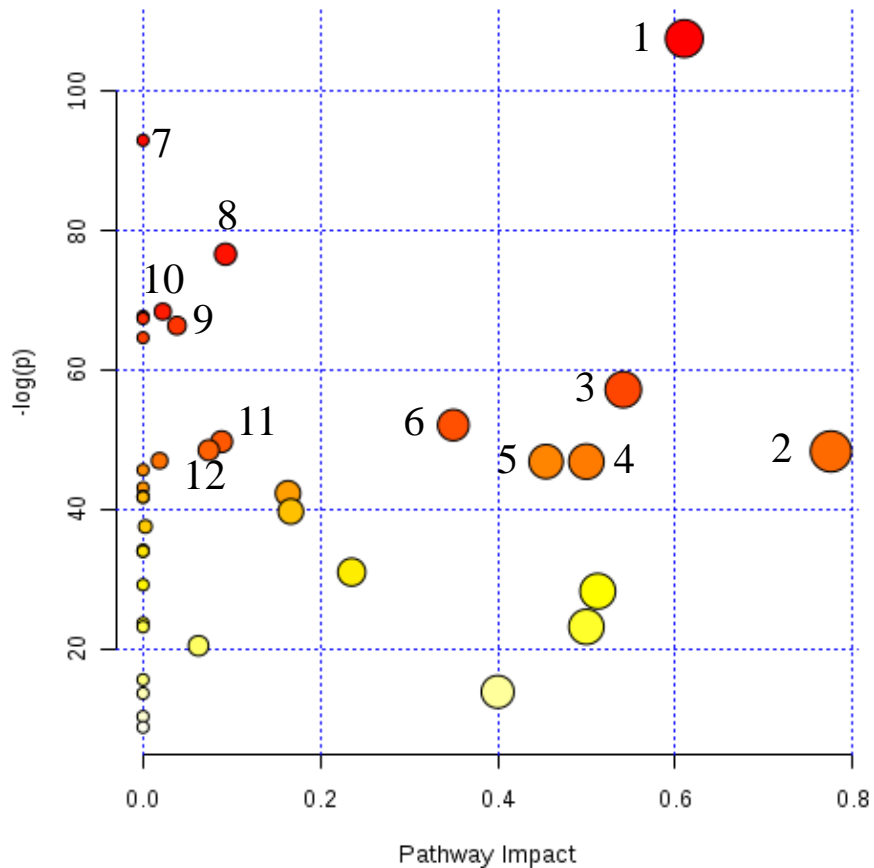
1	Glycine, serine and threonine metabolism
2	Alanine, aspartate and glutamate metabolism
3	Beta alanine metabolism
4	Isoquinoline alkaloid biosynthesis
5	Tyrosine metabolism
6	Pantothenate and CoA biosynthesis
7	Carbon fixation in photosynthetic organisms
8	Aminoacyl-tRNA biosynthesis
9	Phenylpropanoid biosynthesis
10	Pyrimidine metabolism
11	Glutathione metabolism
12	Lysine biosynthesis

Figure 4

Glycine, serine and threonine metabolism

Figure 5

Tryptophan metabolism

Tryptophan → Tryptamine → Serotonin → N-methyl-tryptamine → 5-hydroxy-N-methyl-tryptamine

Serotonin → 5-hydroxy-N-methyl-tryptamine
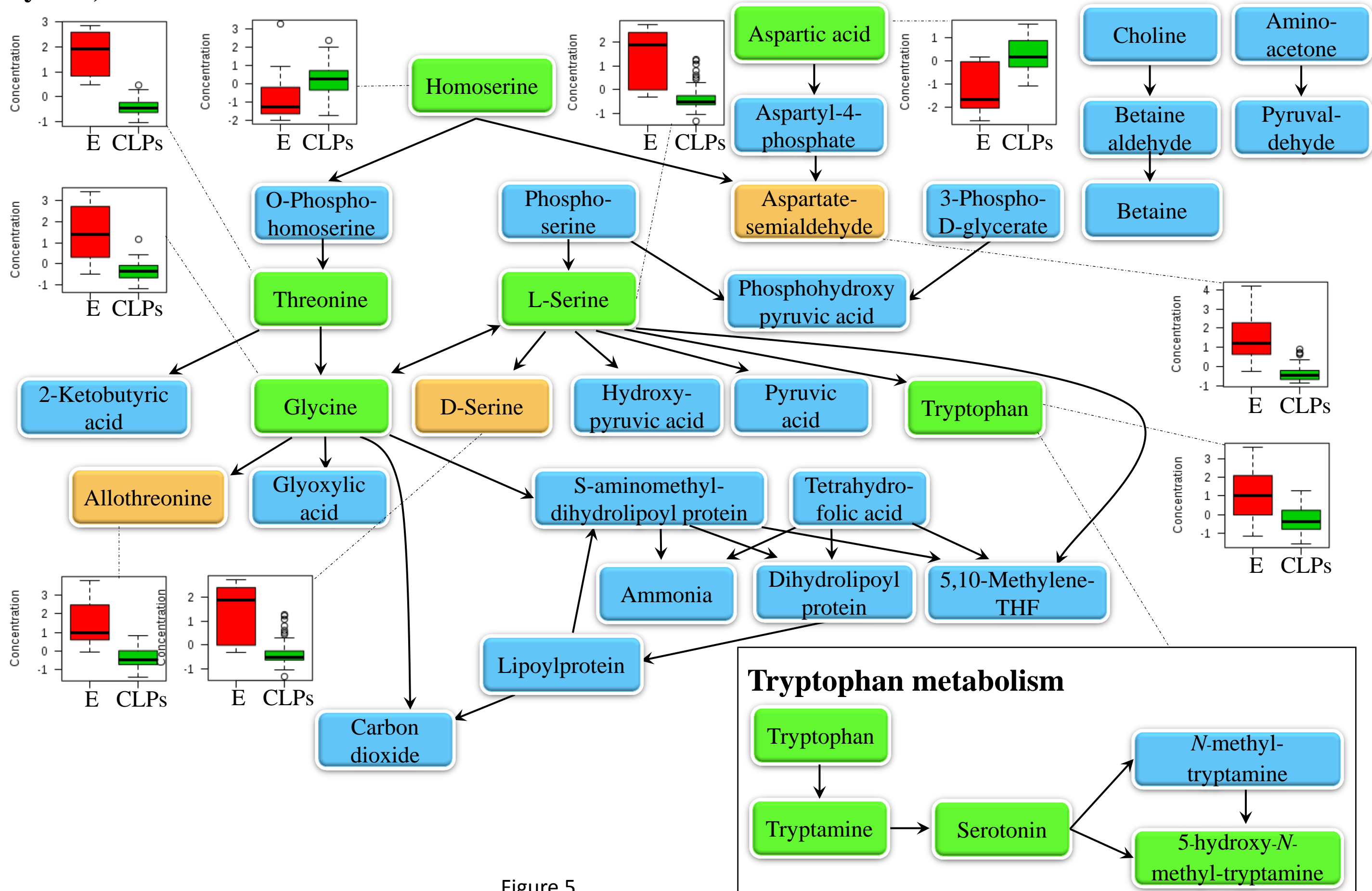
Tyrosine metabolism
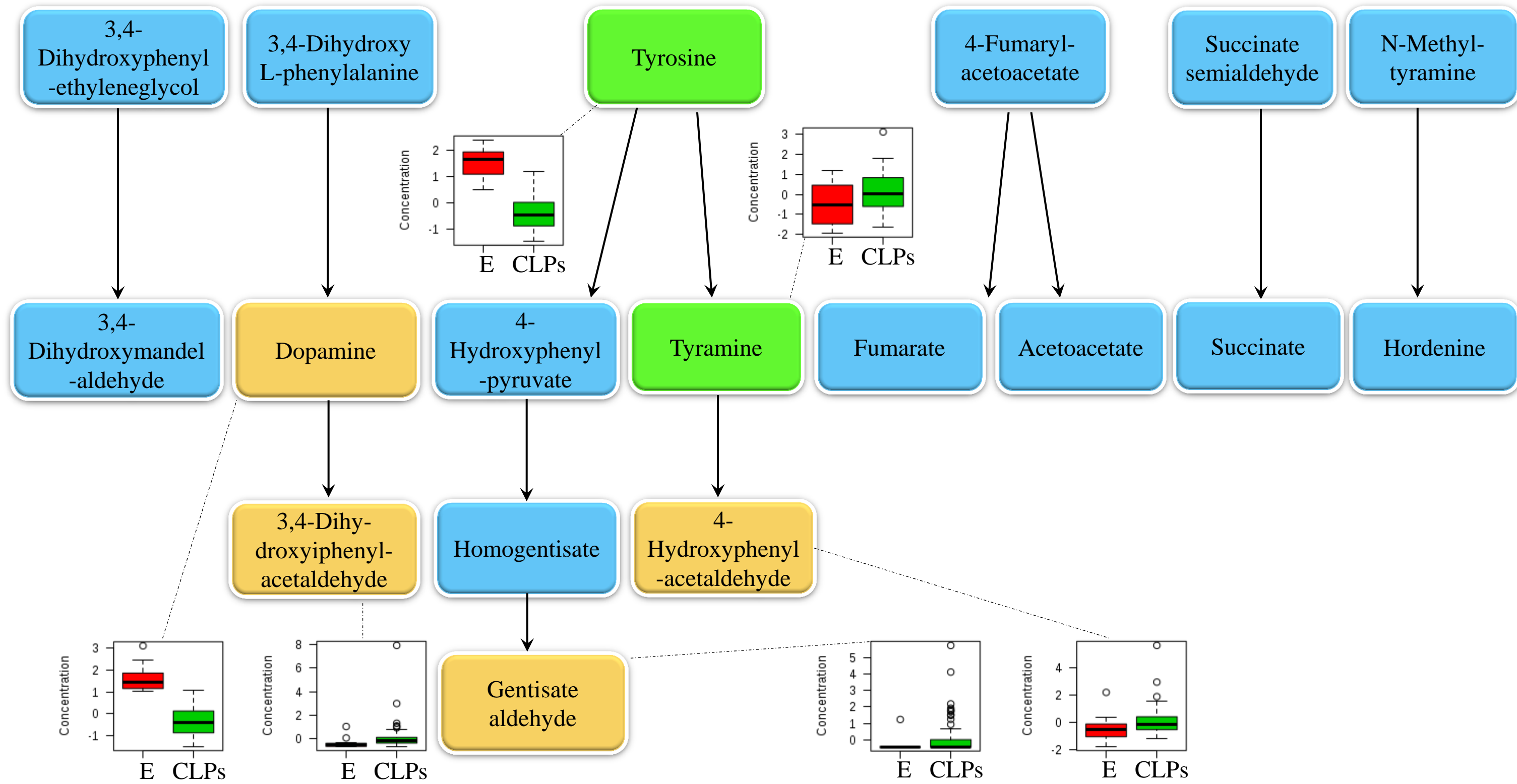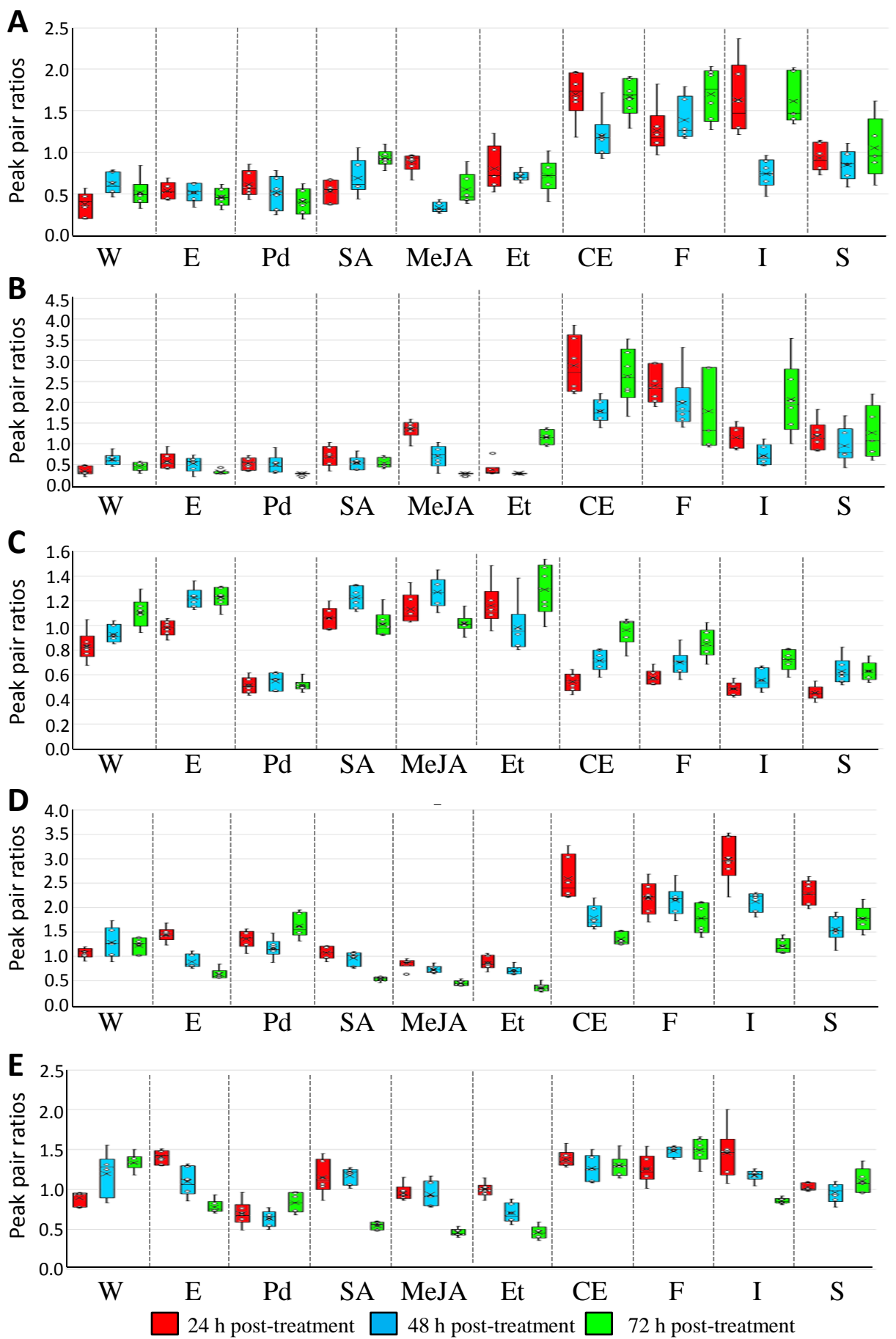
Figure 6

Figure 7
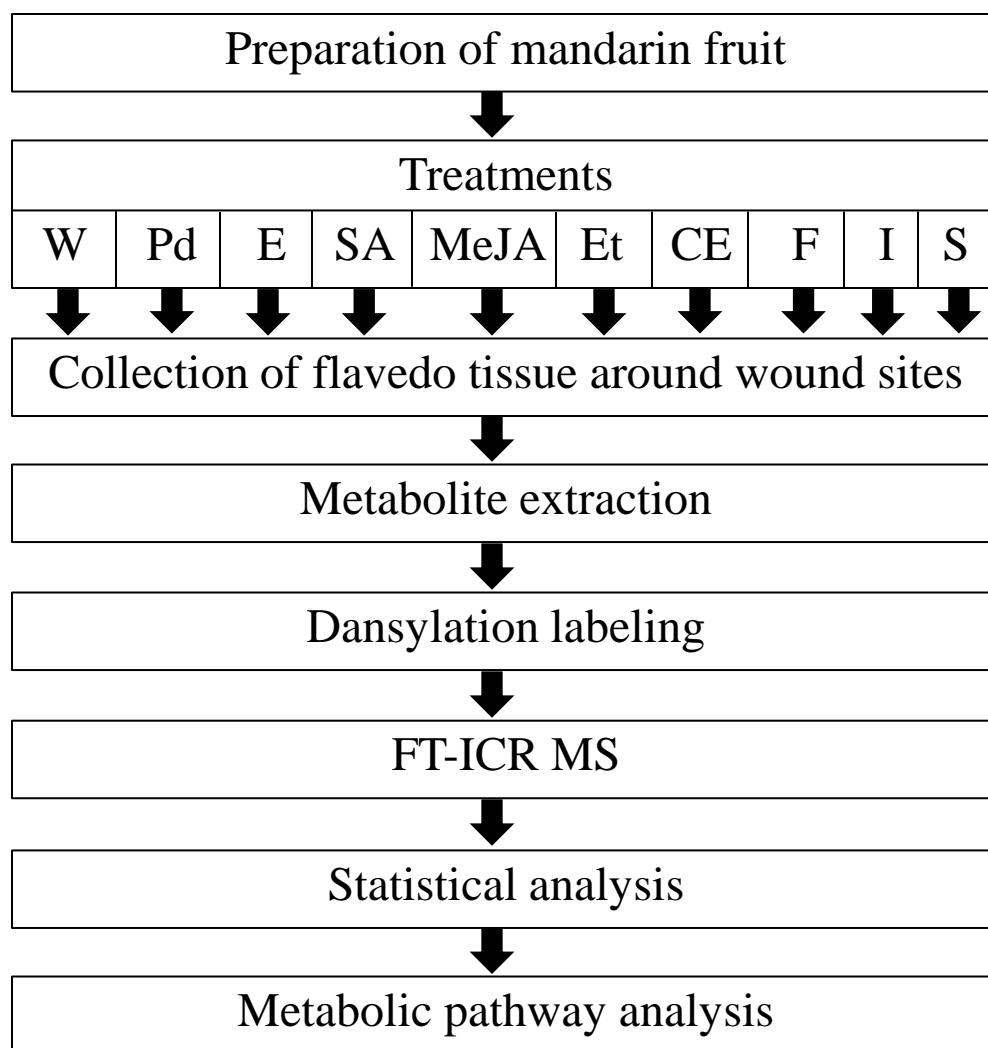
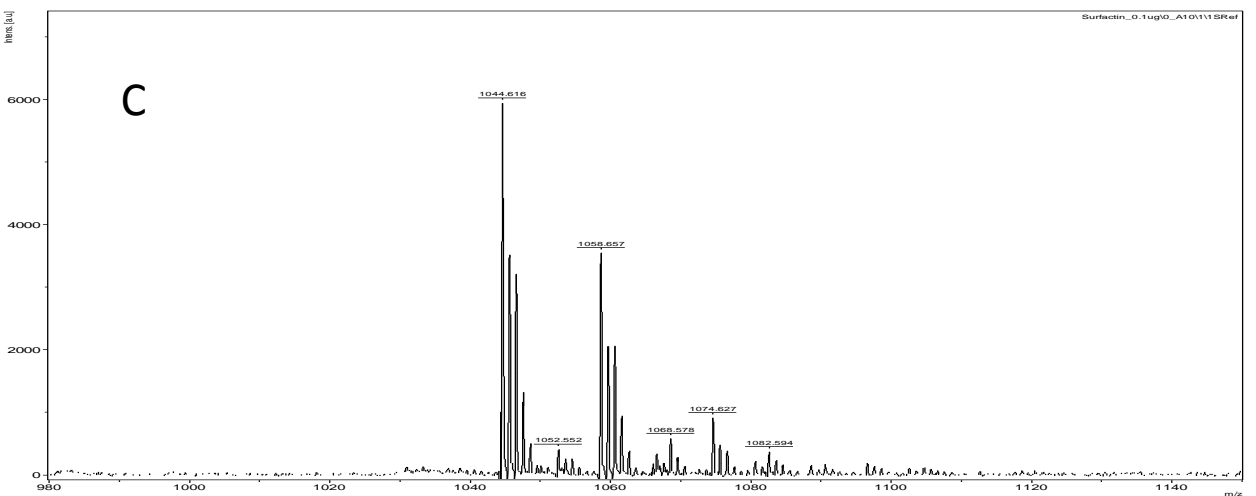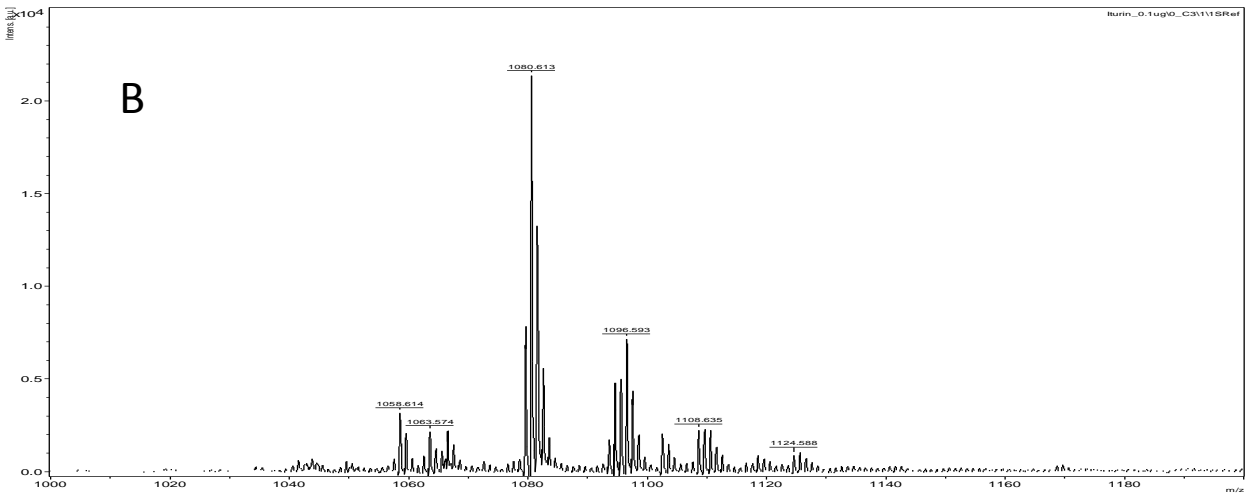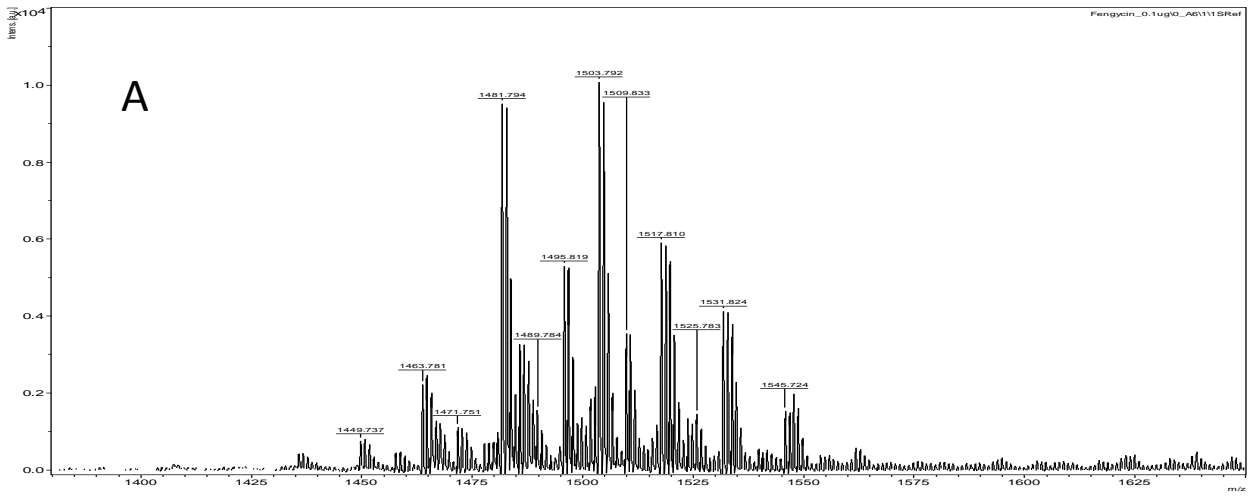Supplementary Fig. 1. Workflow of the study in the treatments of sterile distilled water (W), *Penicillium digitatum* (Pd), ethanol (E), salicylic acid (SA), methyl jasmonate (MeJA), ethephon (Et), CLP extract (CE), fengycin (F), iturin A (I), and surfactin (S).
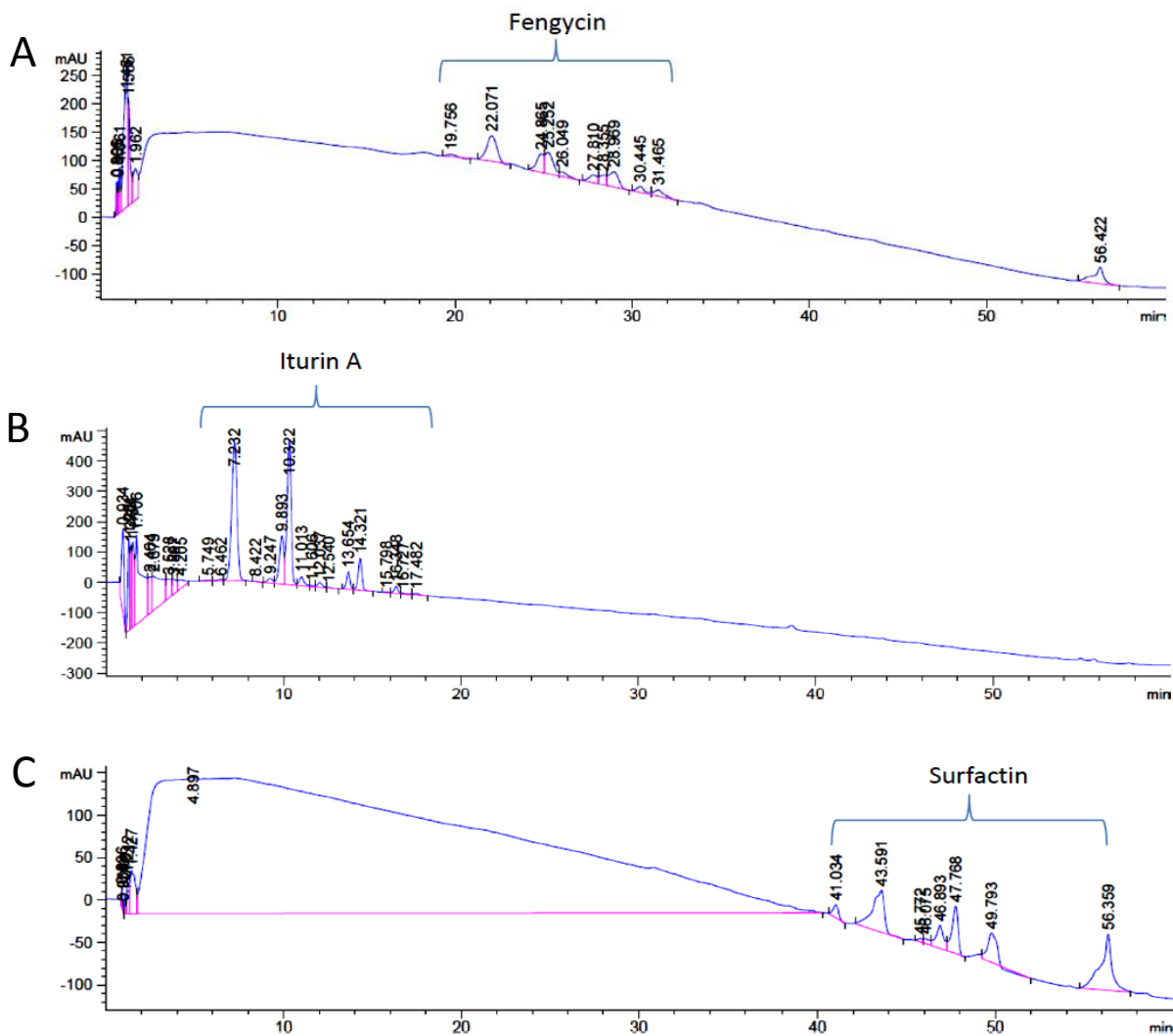
Supplementary Fig. 2. HPLC-UV analysis of bacterial CLPs.

Supplementary Fig. 3. MALDI-TOF MS spectra of bacterial CLPs.
Details such as peak masses can be visualized by enlarging the figure.
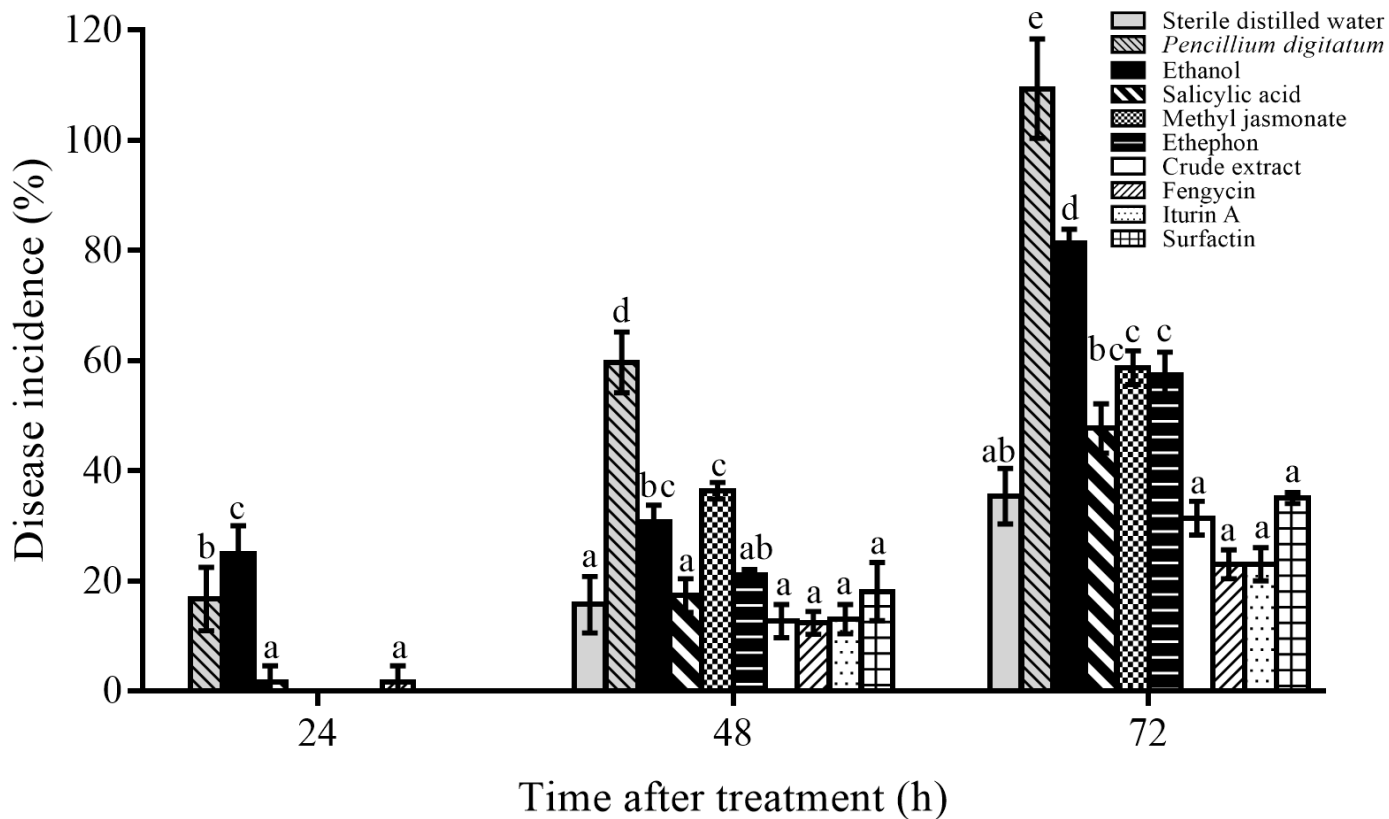
Supplementary Fig. 4. Disease incidence in mandarin fruit of various treatments. Error bars represent standard errors of the mean value of three trials. Bars with the same letter above them show no significant difference to each other using a criterion of $p \leq 0.05$ as significant difference according to Tukey's range test. For example, all the bars marked with "a" in the group of 48 hours after various treatments do not show significant differences.
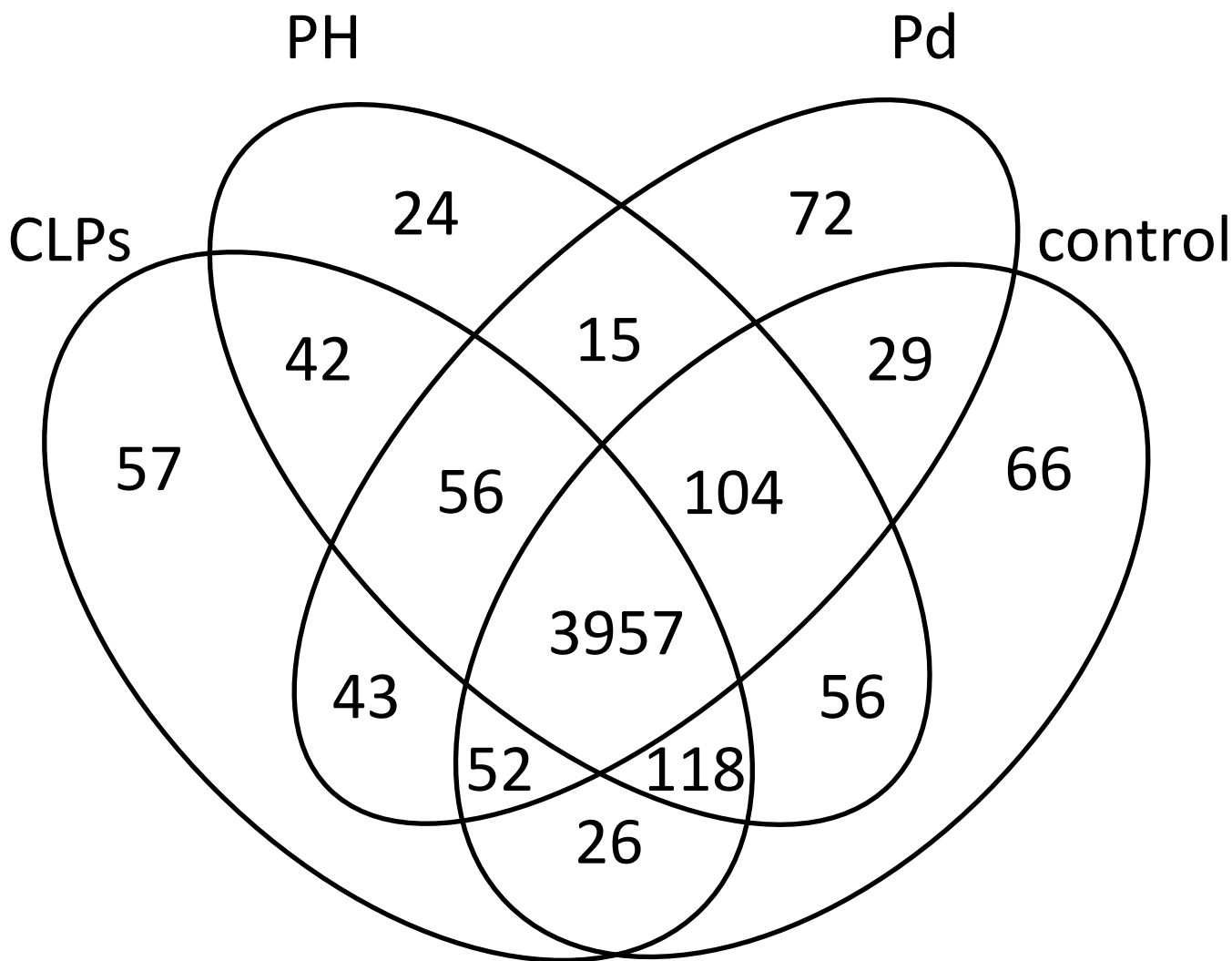
Supplementary Fig. 5. Venn diagram showing the metabolite number distribution in the four major groups of treatments. C, control stress; CLPs, cyclic lipopeptide group; PH, exogenous plant hormones; Pd, *Penicillium digitatum*.